

Supplementary Information for

External light activates hair follicle stem cells through eyes via an ipRGC-SCN-sympathetic neural pathway

Sabrina Mai-Yi Fan, Yi-Ting Chang, Chih-Lung Chen, Wei-Hung Wang, Ming-Kai Pan, Wen-Pin Chen, Wen-Yen Huang, Zijian Xu, Hai-En Huang, Ting Chen, Maksim V Plikus, Shih-Kuo Chen*, Sung-Jan Lin*

*Corresponding authors
Email: alenskchen@ntu.edu.tw and drsclin@ntu.edu.tw

This PDF file includes:

Materials and Methods
Figs. S1 to S7

SI Materials and Methods

Histology and immunofluorescence. Antigen retrieval as suggested by the antibody manufactures was performed. Controls were treated the same, but without primary antibodies. The following antibodies were used: rat anti-BrdU (1:250, Abcam, ab6326), mouse anti-cytokeratin 15(1:200, ThermoFisher Scientific, MA1-90929), Alexa Fluor 488-AffiniPure goat anti-rat IgG (1:500, Jackson ImmunoResearch 112-545-003), CyTM3 AffiniPure donkey anti-mouse IgG (1:500, Jackson ImmunoResearch 715-165-151). Histological images were taken with a light microscope (Nikon, NIE) and fluorescence images were taken with a confocal microscope (Zeiss LSM880, Zeiss, Germany).

For cryostat thick sections, the skin samples were fixed in 4% paraformaldehyde (PFA) in PBS overnight, embedded in Tissue-Tek O.C.T. Compound (Sakura Finetek, USA) and sectioned (100 μ m in thickness) in the cryostat. The section samples were serially dehydrated with sequential replacement of 50%, 75%, 95%, 99% ethanol for 5 minutes and kept in xylene for 5 minutes. The xylene-treated skin was washed with 99% ethanol for three times and rehydrated with 95%, 75%, 50% ethanol and water for 5 minutes at each step. The sections were incubated with blocking reagent PBST (PBS, 1% Tween 20 (Bio Basic, Canada)) with 5% bovine serum albumin (BSA, AMRESCO, USA) for 2 hours and then in primary antibody solution for 2 days at 4 $^{\circ}$ C with gentle shake (40 rpm). The section skin samples were washed with 1mL PBST for 1 hour three times at room temperature and incubated with secondary antibody solution with DAPI (Sigma, USA) for immunofluorescence staining and nuclear labeling for 24hours. The antibodies used were as follows: sheep anti-tyrosine hydroxylase (1:200, Millipore, USA), rabbit anti-cytokeratin 5(1:200, Abcam, ab52635), mouse anti-cytokeratin 15,

mouse anti-alpha smooth muscle actin antibody (1:400, Sigma, C6198), rabbit anti- β 2-adrenergic receptor (1:100, Alomone Labs, AAR-016), CyTM3 AffiniPure donkey anti-sheep IgG (H+L), CyTM3-AffiniPure Goat anti-rabbit IgG (1:500, Jackson ImmunoResearch 111-165-144), CyTM3 AffiniPure donkey anti-mouse IgG (1:500, Jackson ImmunoResearch 715-165-151) and Alexa Fluor® 488 AffiniPure donkey anti-chicken IgG (1:500, Jackson ImmunoResearch 703-545-155). After 24 hours, the skin samples were washed with PBST for an hour three times at room temperature and mounted with fluorescence mounting medium (Dako, Denmark). Controls were treated the same, but without primary antibodies. The images were acquired with a confocal microscope (Zeiss LSM880, Zeiss, Germany) and the z section was 1 μ m. Images were rendered by compressing 34 serial z sections with 1 μ m intervals by Avizo software (Thermo, USA.).

For detection of sympathetic innervation to HFs before and after sympathetic denervation, the skin specimen of 7-week old normal female mice was used for comparison with the experimental groups. For the detection of β 2-adrenergic receptor distribution in HFs, interfollicular epidermis that has been shown to be positive for β 2-adrenergic receptors was used for comparison. For analysis of cell proliferation state in HFs by pulse BrdU labeling, female mice of the age of 19-20 days (telogen) and 30-31 days (anagen) with or without BrdU labeling were used for comparison. In serial immunofluorescent sections, about 25-35 HFs were imaged for analysis in each sample.

To quantify ipRGCs in retina, after the light irradiation experiments (~10 weeks old), wild-type and *Opn4^{tda/+}* mice were perfused with 45ml of 4% PFA, and the retina was dissected out. Whole-mount retina was post-fixed for two overnights at 4°C, and

incubated with blocking solution (0.2% Triton X-100 and 5% normal goat serum in PBS) for two hours at room temperature. Retina was stained with melanopsin primary antibody (rabbit anti-melanopsin, 1:2000, Advanced Targeting Systems) overnight at 4°C and washed with PBS six times for 1 hour. Retina was incubated with a secondary antibody (1:500, Biotium, CF488A goat anti-rabbit IgG) overnight at 4°C and mounted in mounting solution (Vectashield mounting medium, Vector Labs). For controls, specimens were treated the same but without primary antibodies. Images were taken with a confocal microscope (Zeiss LSM880, Zeiss, Germany).

Recordings and analysis of renal sympathetic nerve activity. The mouse was sedated by isoflurane induction and remained anaesthetized with a mixture of zolazepam (Zoletil vet, Virbac Laboratories) and xylazine (Rompun, Bayer) (4:1, v/v) on a temperature-controlled heat pad at 37°C during the whole procedure. The eyes were covered to prevent accidental light exposure before stimulation with light emitting diodes. The retroperitoneal space of the kidney on one side was exposed, and the renal sympathetic nerve was identified at the hilar region. Two platinum electrodes, serving as recording and reference electrodes, were placed 3 mm apart, hooked on the nerve and isolated from other body parts with mineral oil (Sigma M5904). The action potentials were recorded as baseline for 8 minutes, and the mouse eyes were exposed to blue light (2J/cm², 8min and 20sec of light exposure). The recordings lasted for an hour. The control group was treated the same without the blue light on. The electrical signals were filtered (300-3,000 Hz band-pass filter), amplified (20,000x), and digitized (sampling rate: 40,000 Hz) with a microelectrode amplifier (Model 3600, A-M System). Signals recorded were processed

off-line by SciWorks 8.0 (DataWave Technology). Action potentials (spikes) were identified by a detecting threshold, which was greater than 2-folds of background noises. The detected spikes underwent a sorting algorithm with principle component analysis (PCA) to isolate signals from different axons as individual single units (1, 2). The isolated single units then underwent a burst detecting algorithm, to identify the reactive cluster firings (bursts) against the intrinsic, tonic firing background of the renal sympathetic nerve. Bursts were identified by interval criteria: maximal interval to start a burst, 20 ms; minimal interval to end a burst, 20 ms; and minimal number of spikes in a burst (1, 2). While the averaged spike-firing rates indicated the tonic sympathetic activities, we also calculated the activation index, which is the ratio of burst rates normalized by the spike-firing rates of each single unit, to reflex the phasic activities of renal sympathetic nerves.

RNA-sequencing and analysis. The cDNA libraries were sequenced from both the 5' and 3' ends by Illumina GA II. The short reads with their adaptor sequences were trimmed and then aligned to UCSC mouse genome version 10 with STAR (3). All the alignment parameters were set with default values. The average alignment rate was ~95%. Data analysis for expression changes was performed by Cufflinks pipeline (4), and the read counts of genes were normalized based on the reads per kilobase per million mapped reads (RPKM). RNA-seq raw data have been submitted to <http://www.ncbi.nlm.nih.gov/geo> (accession no. GEO: GSE98668). More details were provided in Table S1. To identify the cellular processes/signaling pathways upregulated in the mouse skin after treatment with light irradiation, genes with greater than 1.5-fold

increase were analyzed by DAVID Bioinformatics Resources 6.7

(<https://david.ncifcrf.gov/>). The significantly upregulated cellular processes/signaling pathways ($p < 0.05$) were selected and ranked by p -values.

Reference

1. Pan MK, *et al.* (2014) Deranged NMDAergic cortico-subthalamic transmission underlies parkinsonian motor deficits. *The Journal of clinical investigation* 124(10):4629-4641.
2. Tai C-H, Yang Y-C, Pan M-K, Huang C-S, & Kuo C-C (2011) Modulation of subthalamic T-type Ca²⁺ channels remedies locomotor deficits in a rat model of Parkinson disease. *The Journal of clinical investigation* 121(8):3289-3305.
3. Dobin A, *et al.* (2013) STAR: ultrafast universal RNA-seq aligner. *Bioinformatics* 29(1):15-21.
4. Trapnell C, *et al.* (2012) Differential gene and transcript expression analysis of RNA-seq experiments with TopHat and Cufflinks. *Nat Protoc* 7(3):562-578.

SI Figures

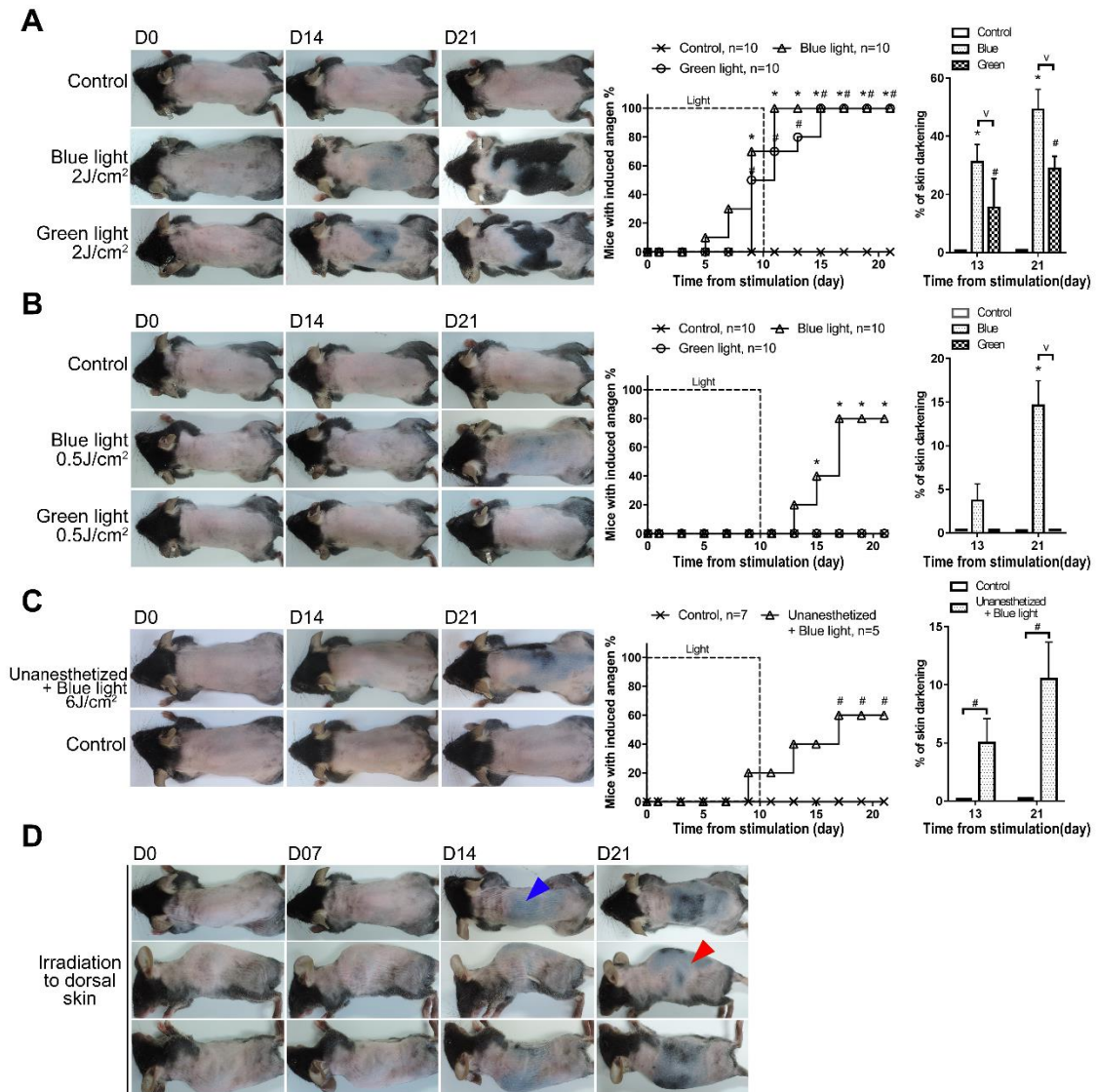


Fig. S1. Effect of optic stimulation with light of different wavelengths and doses on hair regeneration and hair regrowth pattern induced by blue light irradiation to skin.

7-week old mice were exposed to daily optic light stimulation at zeitgeber time ZT1-2 for 10 consecutive days. Blue light (463±50nm) or green light (522 ±50nm) were used. (A-C) Irradiation to eyes. (D) Irradiation to dorsal skin. (A) Effect of blue or green light at

2J/cm² per day under anesthesia. Both blue and green light promoted anagen entry. **p*<0.05 (n=10), blue light vs. non-irradiated control. # *p*<0.05 (n=10), green light vs. non-irradiated control. v *p*<0.05 (n=10), blue light vs. green light. **(B)** Effect of blue or green light at 0.5J/cm² per day under anesthesia. Blue light at this level still induced anagen entry, but anagen induction was delayed compared with blue light at 2J/cm² per day. Green light did not induce anagen entry at this dose. * *p*<0.05 (n=10), blue light vs. non-irradiated control. v *p*<0.05 (n=10), blue light vs. green light. **(C)** Effect of blue light at 6J/cm² per day in the unanesthetized condition. Compared with non-irradiated control, premature anagen entry was also induced by blue light in the unanesthetized condition. # *p*<0.05 (n=7 for control, 5 for blue light irradiation). **(D)** Pattern of anagen induction by direct blue light irradiation to dorsal skin. Mice were irradiated by blue light 2J/cm² each day for 10 consecutive days. Anagen entry was first observed homogeneously on the back (D14, blue arrowhead) and then extended to the lateral trunk (D21, red arrowhead).

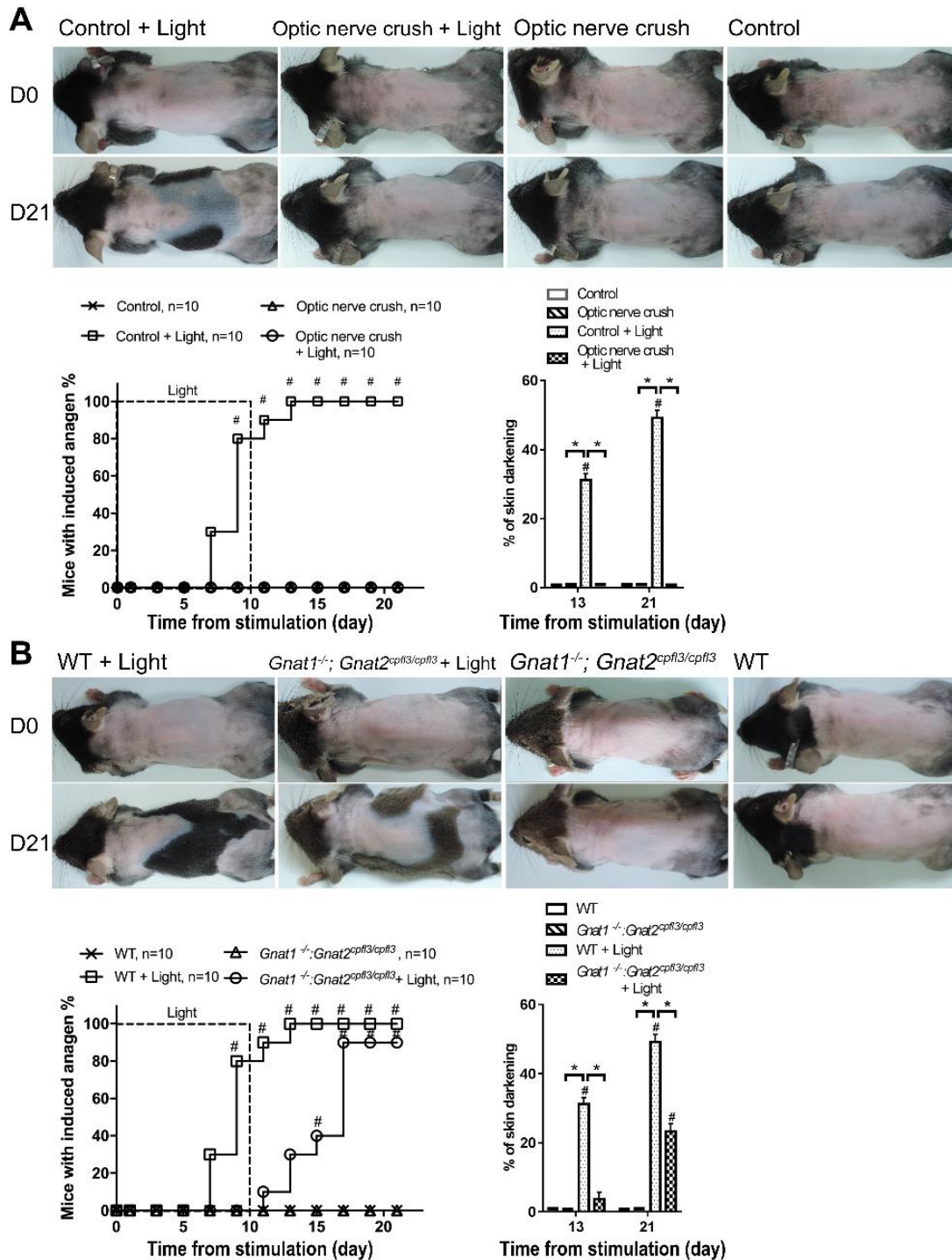


Fig. S2. Intact optic nerves are required while cones and rods are dispensable for light-induced anagen entry.

(A) Optic nerves of both eyes were crushed before light stimulation. Blue light-induced anagen entry was completely inhibited when optic nerves were crushed. # $p < 0.05$ (n=10),

compared with non-irradiated control. * $p < 0.05$ (n=10), Control+light vs. optic nerve crush or optic nerve crush+light. **(B)** $Gnat1^{-/-}; Gnat2^{cpfl3/cpfl3}$ mice were stimulated with daily blue light. Although anagen induction was delayed compared with wild-type mice, premature anagen entry was still observed in $Gnat1^{-/-}; Gnat2^{cpfl3/cpfl3}$ mice after blue light stimulation. It is of note that, after light stimulation, the area of anagen entry was greater in wild type mice than $Gnat1^{-/-}; Gnat2^{cpfl3/cpfl3}$ mice on both day 13 and day 2. # $p < 0.05$ (n=10), compared with non-irradiated control. * $p < 0.05$ (n=10), WT+light vs. $Gnat1^{-/-}; Gnat2^{cpfl3/cpfl3}$ or $Gnat1^{-/-}; Gnat2^{cpfl3/cpfl3}$ +light. WT: wild type.

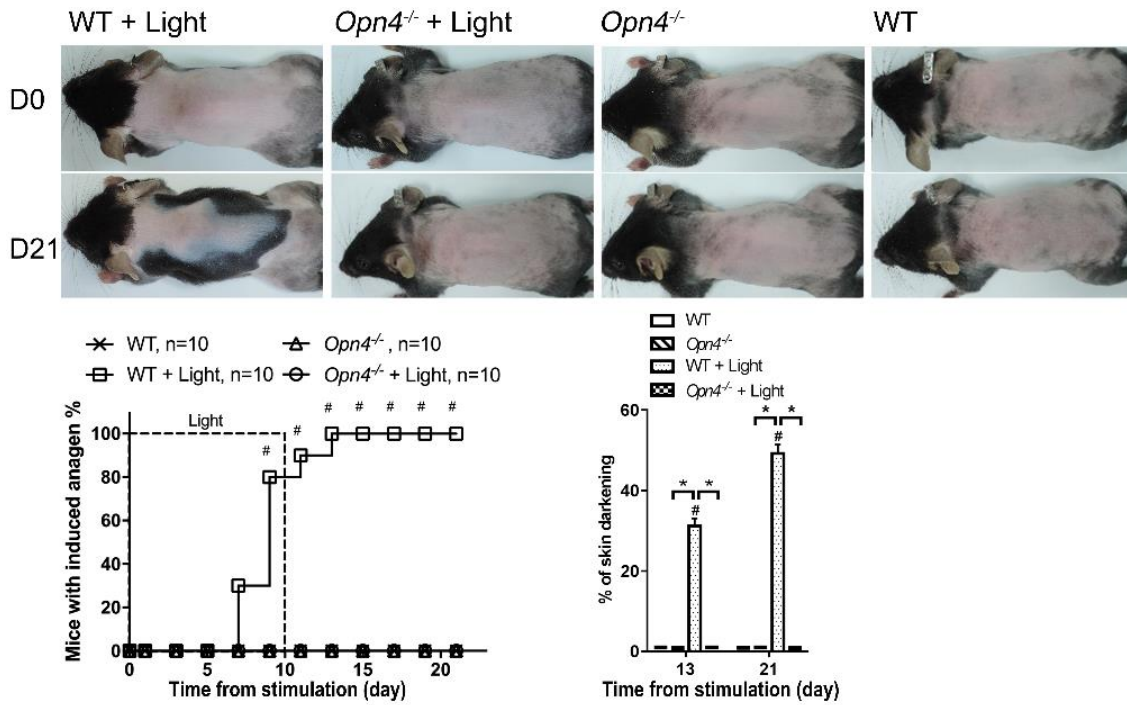


Fig. S3. Melanopsin is required for light-induced anagen entry.

Optic blue light stimulation failed to induce anagen entry in *Opn4*^{-/-} mice. # $p < 0.05$

($n = 10$), compared with non-irradiated wild-type control. * $p < 0.05$ ($n = 10$), WT+light vs.

Opn4^{-/-} or *Opn4*^{-/-}+light. WT: wild type.

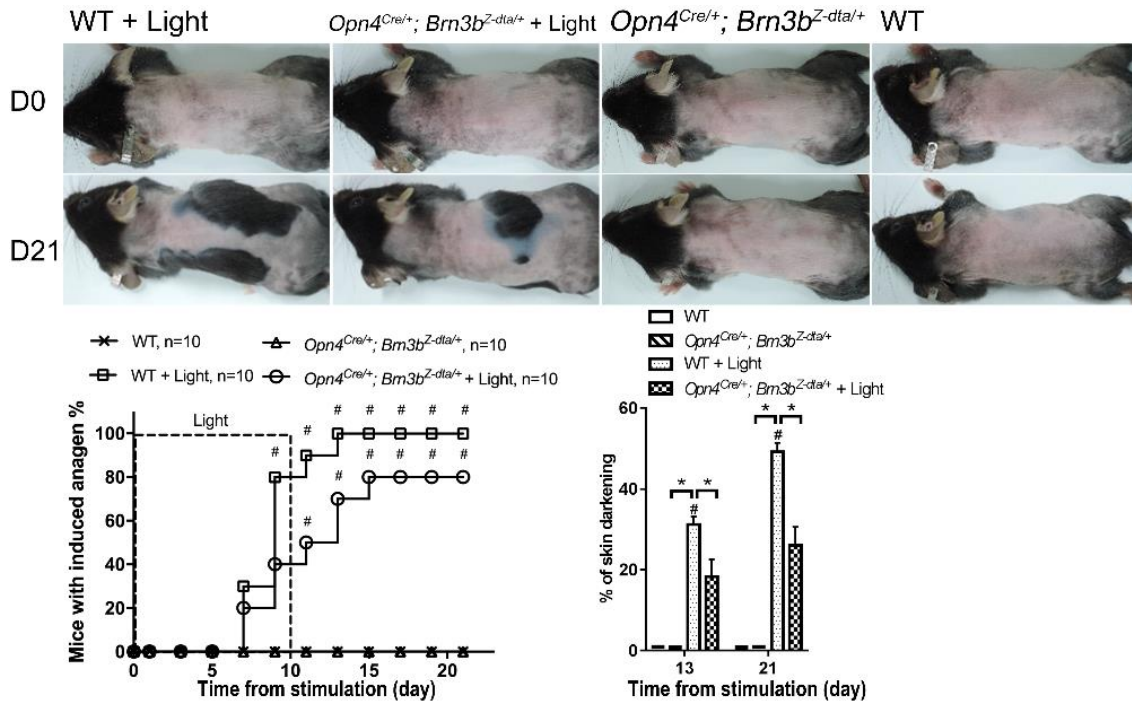


Fig. S4. Effect of light stimulation on *Opn4^{Cre/+}; Brn3b^{Z-dta/+}* mice.

In *Opn4^{Cre/+}; Brn3b^{Z-dta/+}* mice, optic blue light stimulation could still induce anagen entry. # $p < 0.05$ (n=10), compared with non-irradiated wild-type mice. * $p < 0.05$ (n=10), WT+light vs. *Opn4^{Cre/+}; Brn3b^{Z-dta/+}* or *Opn4^{Cre/+}; Brn3b^{Z-dta/+}*+light. WT: wild type.

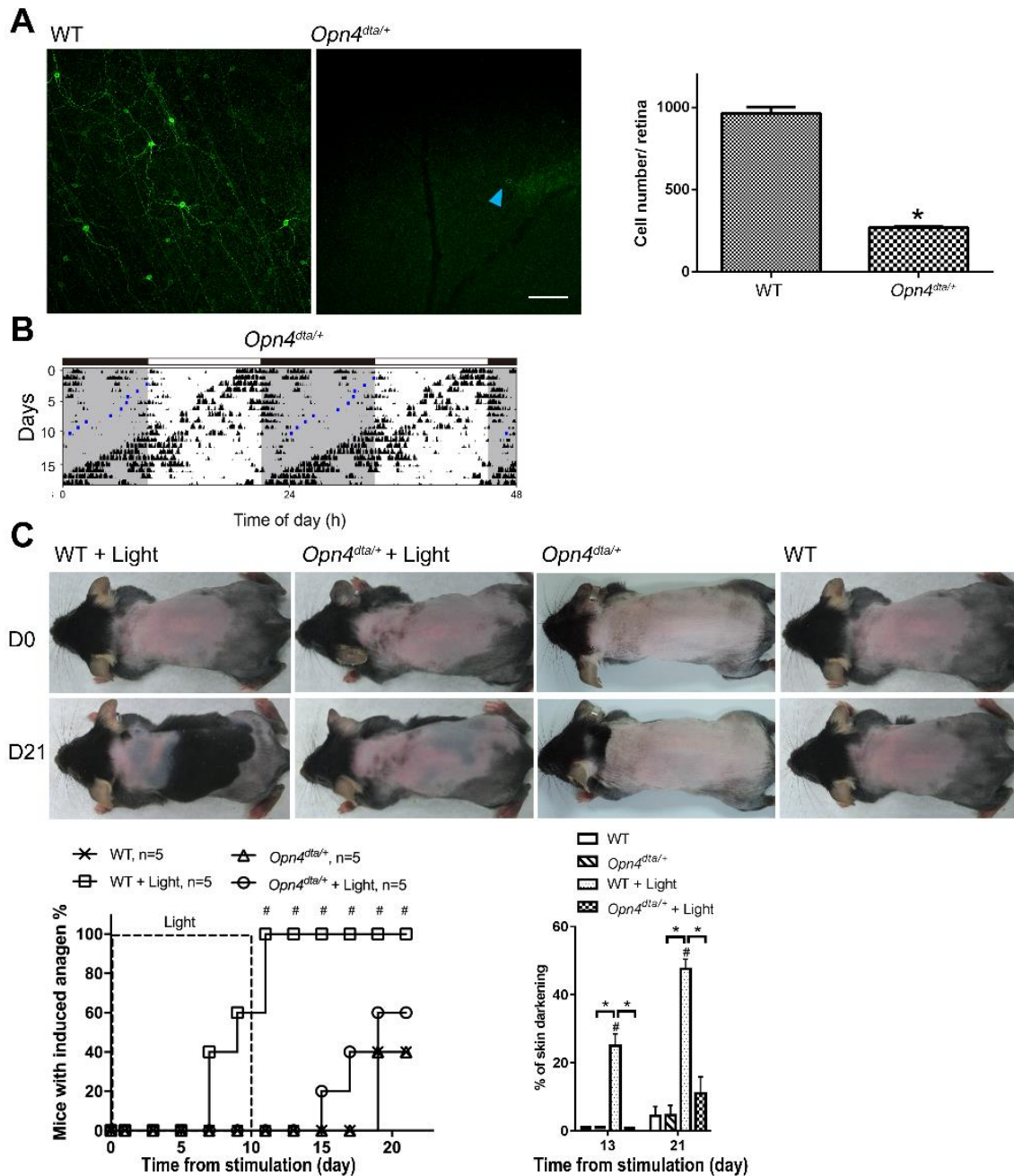


Fig. S5. Effect of optic blue light stimulation on mice with M1 ipRGCs elimination.

(A) Immunostaining and quantification of ipRGCs. ipRGCs were detected by immunostaining for melanopsin after the light irradiation experiment (~ 10 weeks old). ipRGCs were significantly reduced in *Opn4^{dta/+}* mice. * $p < 0.05$ (n=3), WT vs. *Opn4^{dta/+}* mice. Most M1 ipRGCs with strong melanopsin signal were not observed in *Opn4^{dta/+}* mice. Only some weakly stained ipRGCs (blue arrowhead, right panel) could be observed

in *Opn4^{dta/+}* mice. Similar results were obtained in three independent experiments.

Bar=100 μ m. **(B)** Wheel running activity and time of light irradiation for *Opn4^{DTA/+}*. The

daily activity was free running due to reduced M1 ipRGCs. Mice were irradiated with

blue light at CT1 (circadian time) indicated by blue color. **(C)** Effect of optic blue light

stimulation on *Opn4^{dta/+}* mice. In *Opn4^{dta/+}* mice, light-induced anagen entry was delayed

and reduced compared with wild-type mice. # $p < 0.05$ (n=5), compared with non-

irradiated wild-type control. * $p < 0.05$ (n=5), WT+light vs. *Opn4^{dta/+}* or *Opn4^{dta/+}*+light.

WT: wild type.

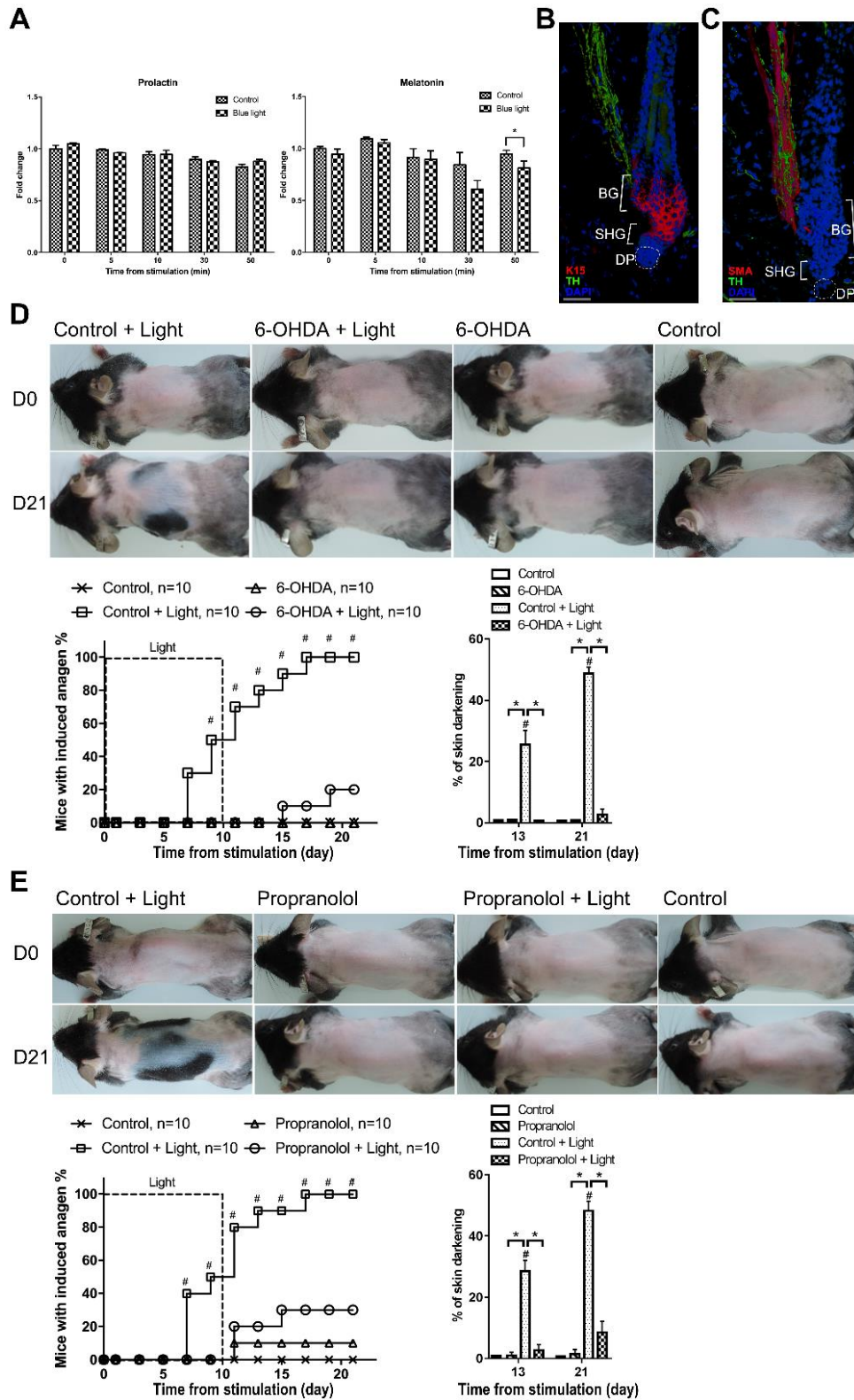


Fig. S6. Effect of blue light on plasma prolactin and melatonin levels, innervation of sympathetic nerves to HF and the role of sympathetic nerves in light-induced

anagen entry.

(A) Plasma prolactin and melatonin level after blue light irradiation. Mice were irradiated by blue light $2\text{J}/\text{cm}^2$ at zeitgeber time ZT1-2. There were no significant differences of prolactin levels between the non-irradiated and irradiated groups. Melatonin was slightly reduced at 50min in the irradiated mice. * $p < 0.05$ (n=3). **(B-C)** Immunostaining. Images were compressed from 34 serial confocal z-images with $1\mu\text{m}$ intervals from cryostat thick sections of 7-week female mice. **(B)** HFSCs are labeled by K15. Sympathetic nerves, positive of tyrosine hydroxylase, are in close proximity to HFSCs. Bar= $50\mu\text{m}$. **(C)** Arrector pili muscles are labeled by α -smooth muscle actin. Sympathetic nerves heavily innervate arrector pili muscle after they leave the HF. TH: tyrosine hydroxylase; SMA: α -smooth muscle actin. Bar= $50\mu\text{m}$. **(D)** Sympathectomy with 6-OHDA. 6-OHDA treatment suppressed light-induced anagen entry. # $p < 0.05$ (n=10), compared with non-6-OHDA-treated non-irradiated control. * $p < 0.05$ (n=10), Control+light vs. 6-OHDA or 6-OHDA+light. **(E)** Effect of β -adrenergic antagonist on light-induced anagen entry. Daily topical propranolol treatment inhibited blue light-induced anagen entry. # $p < 0.05$ (n=10), compared with non-propranolol-treated non-irradiated control. * $p < 0.05$ (n=10), Control+light vs. propranolol or propranolol+light.

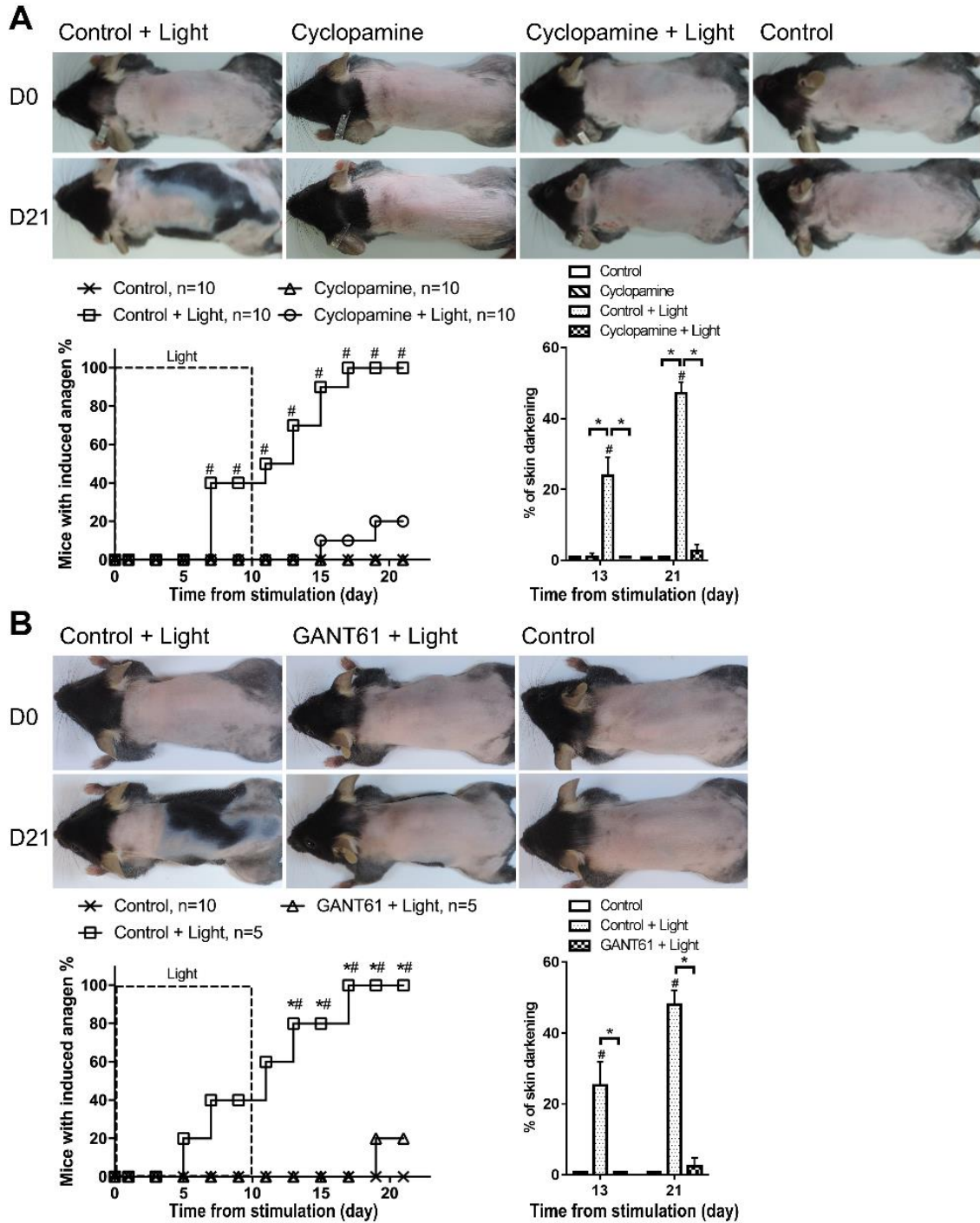


Fig. S7. The role of hedgehog signaling in light-induced anagen entry.

(A) Effect of Smoothed inhibitor on light-induced anagen entry. Topical treatment with cyclopamine that inhibits Smoothed suppressed blue light-induced anagen entry. #

$p < 0.05$ (n=10), compared with non-cyclopamine-treated non-irradiated control. * $p < 0.05$

(n=10), Control+light vs. cyclopamine or cyclopamine+light. **(B)** Effect of Gli1/2 inhibitor on light-induced anagen entry. Topical treatment with GANT61 that inhibits Gli1/2 suppressed blue light-induced anagen entry. # $p < 0.05$, compared with non-GANT61-treated non-irradiated group. * $p < 0.05$, compared with GANT61-treated irradiated group. n=10 for control, 5 for GANT61+light, 5 for light only.